Discussion Paper No.340

Delay Solow Model with a CES Production Function

Akio Matsumoto
Chuo University

Ferenc Szidarovszky
Corvinus University

January 2021

INSTITUTE OF ECONOMIC RESEARCH
Chuo University
Tokyo, Japan

Delay Solow Model with a Normalized CES Production Function*

Akio Matsumoto† Ferenc Szidarovszky‡

Abstract

This study is aimed at analyzing the relationship between the elasticity of substitution and the birth of cyclic macro-dynamics. We first normalize a CES production function that consistently involves all its variants. Introducing two different delays, called a gestation delay and a depreciation delay, into the Solow model, we then find that the gestation delay alone does not affect the stability of the balanced growth equilibrium. Third, we construct the stability switching curve that separates the stable and unstable regions in the plane of the two delays and derive the stability index to confine whether the stability is lost or gained when the two delays cross the curve. Lastly, we numerically demonstrate that appropriate combinations of two delays can be a source of oscillatory fluctuations.

Keywords: Normalized CES production function, Solow model, Gestation delay, Depreciation delay, Stability switching curve

*The first author highly acknowledges the financial supports from the Japan Society for the Promotion of Science (Grant-in-Aid for Scientific Research (C) 20K01566). The usual disclaimers apply.

†Professor, Department of Economics, Chuo University, 742-1, Higashi-Nakano, Hachioji, Tokyo, 192-0393, Japan. akiom@tamacc.chuo-u.ac.jp

‡Professor, Department of Mathematics, Corvinus University, Budapest, Fövám tér 8, 1093, Hungary. szidarka@gmail.com

1 Introduction

In the recent literature, it is demonstrated that traditional growth models might be cyclic if time delays are introduced. See Tsuzuki (2016) for a new Keynesian model, Gori et al. (2017) for a Keynesian model, Guerri et al. (2019) and Matsumoto and Szidarovszky (2020) for a Solow model and an extended Solow model augmented with human capital. This finding indicates that delay growth models could explain the cyclic behavior of various economic variables. On the other hand, in the existing growth literature, there has been a rising interest on the relation between factor substitution and economic growth. In consequence, in view of a systematic comparison between production technologies and various elasticity of factor substitution, a normalized CES production function has been developed (see for example Klump and Preissler (2000)). Nevertheless, little is known about dynamic behavior of a delay Solow model having a CES production function. This study investigates the conditions under which the delay Solow model gives rise to oscillatory fluctuations. The model is delayed because it involves a gestation delay of investment and a depreciation delay of capital stock. Beside, it adopts a normalized CES production function.

The Solow model with no delays concerns the long-run evolution of the economy. After the economy reaches its steady state, it describes from a more long-run point of view how per-capita output grows via exogenous factors changes such as population growth, technological progress and the saving rate. On the other hand, oscillatory fluctuations that are the main concern of macroeconomics are often observed in a real economy. In his classic development of the theory of business cycle, Kalecki (1935) discovers that a delay of investment called a gestation delay could be the main source of macro-cyclic dynamics. In the early 50s, Hicks (1950) and Goodwin (1951) credit macro-cycles with nonlinearities.[1] In later periods, Day (1982) gets down to the nitty-gritty of nonlinearity and shows that the Solow model with nonlinear production function depending on the influence of pollution can generate complex dynamics involving chaos in a discrete-time framework. Matsumoto and Szidarovszky (2011) reconsider Day's discrete time model in a continuous-time framework and show the birth of chaotic dynamics if the delay in investment becomes strong enough. It conveys a new result that nonlinearities and the delay could be responsible for the birth of chaotic dynamics in continuous-time models.

This study is a continuation of Guerrini et al. (2019) that consider the same model with a Cobb-Douglas production function and determine the stability switching curve on which stability is lost or gained. Its main purpose is to make clear the relation between the elasticity of factor substitution and the stability-loss-and-gain. The main results are the followings:

(i) Complex dynamics can emerge more likely if the elasticity of substitution is smaller;

[1] Goodwin's model (1951) has a delay due to the acceleration principal, however, his main dynamic equation is linearized at the zero-delay point and thus gets rid of the influence caused by delay. The existence of a limit cycle is mainly due to the nonlinearities of the investment function.

(ii) Multiple stability switches can occur if the elasticity of substitution is larger than unity.

The rest of the paper is organized as follows. Section 2 constructs a normalized CES production function that includes all variants. Section 3 reviews the Solow model with no-delays and examines the dynamic properties of the Solow model with one delay. Section 4 extends the model by introducing two different delays and analytically derives the stability switching curve. Finally, concluding remarks and further research directions are given in Section 5.

2 Normalized CES Production Function

Let $Y = F(K, L)$ be a production function having two inputs, capital K and labor L, F_K and F_L are the marginal products of capital and labor, F_{KL} is the cross derivative. The two definitions of the elasticity of substitution between capital and labor were given, independently, by Hicks (1932, p.244) and Robinson (1933, p.256). The formulation defined by Hicks (1932) is as follows:

$$\sigma_H = \frac{F_K F_L}{F_{KL} Y}. \tag{1}$$

The economic implication of this definition is not clear. The other formulation by Robinson (1933) is

$$\sigma_R = \frac{d \log (K/L)}{d \log (F_L/F_K)} \tag{2}$$

where the elasticity of substitution is defined as the relative change in the capital-labor ratio against a one percent change in the marginal rate of technical substitution. It has been well-known that these definitions are equivalent if the production function has only two input factors and is homogeneous of degree one, furthermore, the market is perfectly competitive.[2] Under the degree-one homogeneity (i.e., $f(k) = F(K/L, 1)$ with $k = K/L$), the elasticity of substitution (2)[3] can be written as

$$\sigma = -\frac{f'(k)\left[f(k) - kf'(k)\right]}{kf(k)f''(k)} \tag{3}$$

where $f'(k)$ and $f''(k)$ are the first and the second derivative of $f(k)$.

The form of the corresponding production function is shown by Arrow et al. (1961). In particular, integration of (3) leads to an aggregate production function in an extensive form,

$$Y = \left[\alpha L^{\psi} + \beta K^{\psi}\right]^{\frac{1}{\psi}} \tag{4}$$

[2] A formal and compact proof shown by Hicks (1963, p.373) is summarized in the Appendix.
[3] Since the equivalence has been shown, we denote the elasticity of substitution by σ.

where α and β are some arbitrary integration constants and the parameter ψ is a proxy of σ,

$$\psi = \frac{\sigma - 1}{\sigma} \text{ for } 0 \leq \sigma \leq \infty \tag{5}$$

implying that ψ strictly increases in σ and $-\infty \leq \psi \leq 1$. Notice that (4) is a solution of (3), the second-order differential equation in k, and has dependency on the initial point. As is fully emphasized by Klump et al. (2012), the elasticity of substitution is defined as a point elasticity and as a natural consequence, the integration constants of (4) could depend on the baseline values. Hence, the normalized CES function depends on three given baseline values:

$$k_0 = \frac{K_0}{L_0}\text{: capital intensity,}$$

$$\mu_0 = \left[\frac{F_L}{F_K}\right]_{0:K=K_0,L=L_0}\text{: the marginal rate of technical substitution}$$

and

$$y_0 = \frac{Y_0}{L_0}\text{: per-capita output.}$$

Denoting the right-hand side of (4) by $F(K, L)$, we have the marginal rate evaluated at the baseline,

$$\left[\frac{F_L}{F_K}\right]_{0:K=K_0,L=L_0} = \frac{\alpha}{\beta}\left(\frac{L_0}{K_0}\right)^{\psi-1} = \mu_0$$

from which

$$\alpha = \mu_0\left(\frac{K_0}{L_0}\right)^{\psi-1}\beta. \tag{6}$$

This α is substituted into (4) and evaluated at the baseline that has, after arranging the terms, the following form,

$$Y_0 = \left[\beta K_0^{\psi-1}\left(K_0 + \mu_0 L_0\right)\right]^{\frac{1}{\psi}}.$$

Solving this equation for β presents

$$\beta = \frac{Y_0^{\psi}}{K_0^{\psi-1}\left(K_0 + \mu_0 L_0\right)}. \tag{7}$$

Substituting (6) and (7) into (4) and, again, arranging the terms yield

$$Y = Y_0\left[\frac{K_0}{K_0 + \mu_0 L_0}\left(\frac{K}{K_0}\right)^{\psi} + \frac{\mu_0 L_0}{K_0 + \mu_0 L_0}\left(\frac{L}{L_0}\right)^{\psi}\right]^{\frac{1}{\psi}}$$

where

$$\frac{K_0}{K_0 + \mu_0 L_0} = \frac{\left(F_K\right)_0 K_0}{\left(F_K\right)_0 K_0 + \left(F_L\right)_0 L_0} = \frac{r_0 K_0}{Y_0}$$

and

$$\frac{\mu_0 L_0}{K_0 + \mu_0 L_0} = \frac{(F_L)_0 L_0}{(F_K)_0 K_0 + (F_L)_0 L_0} = \frac{w_0 L_0}{Y_0}.$$

Here r_0 and w_0 are the rate of return and the real wage rate, both having output as numéraire and satisfy the profit maximizing conditions,

$$r_0 = (F_K)_0 \text{ and } w_0 = (F_L)_0 .$$

Let π_0 be the capital share in the total income at the point of normalization, then

$$\pi_0 = \frac{r_0 K_0}{Y_0} \text{ and } 1 - \pi_0 = \frac{w_0 L_0}{Y_0}.$$

Hence, the normalized CES production function has the following form:

$$Y = F(K, L) = Y_0 \left[\pi_0 \left(\frac{K}{K_0} \right)^{\psi} + (1 - \pi_0) \left(\frac{L}{L_0} \right)^{\psi} \right]^{\frac{1}{\psi}}. \tag{8}$$

It is well-known that the CES function includes the three most known forms of production technologies as its special cases: The linear production technology when $\psi \to 1$ (i.e., $\sigma \to \infty$),

$$Y = Y_0 \left[\pi_0 \left(\frac{K}{K_0} \right) + (1 - \pi_0) \left(\frac{L}{L_0} \right) \right],$$

the Cobb-Douglas technology when $\psi \to 0$ (i.e., $\sigma \to 1$),

$$Y = Y_0 \left(\frac{K}{K_0} \right)^{\pi_0} \left(\frac{L}{L_0} \right)^{1-\pi_0},$$

and the Leontief technology when $\psi \to -\infty$ (i.e., $\sigma \to 0$).

$$Y = Y_0 \min \left[\frac{K}{K_0}, \frac{L}{L_0} \right].$$

Under the linear homogeneity of the function $F(K_t, L_t)$, the corresponding intensive form of (8) is

$$y = f(k) = y_0 \left[\pi_0 \left(\frac{k}{k_0} \right)^{\psi} + (1 - \pi_0) \right]^{\frac{1}{\psi}} \tag{9}$$

where

$$y = \frac{Y}{L},\ k = \frac{K}{L} \text{ and } f(k) = F\left(\frac{K}{L}, 1 \right).$$

The intensive forms in the special cases are

$$y = y_0 \left[\pi_0 \left(\frac{k}{k_0} \right) + (1 - \pi_0) \right] \text{ when } \psi \to 1,$$

$$y = y_0 \left(\frac{k}{k_0} \right)^{\pi_0} \text{ when } \psi \to 0,$$

$$y = y_0 \min \left[\frac{k}{k_0}, 1 \right] \text{ when } \psi \to -\infty.$$

We will take the following specification of the baseline whenever we give numerical examples. Under Assumption 1, Figure 1(A) depicts the three different shapes of the isoquants, $F(K, L) = Y_0$, with the different values of ψ while Figure 1(B) represents the graphs of the corresponding intensive forms. It is seen in both figures that the curves pass the common baseline values denoted by the black points and are tangent to each other there.

Assumption 1. $Y_0 = 1,\ K_0 = 1,\ L_0 = 2$ and $r_0 = 1/3$.

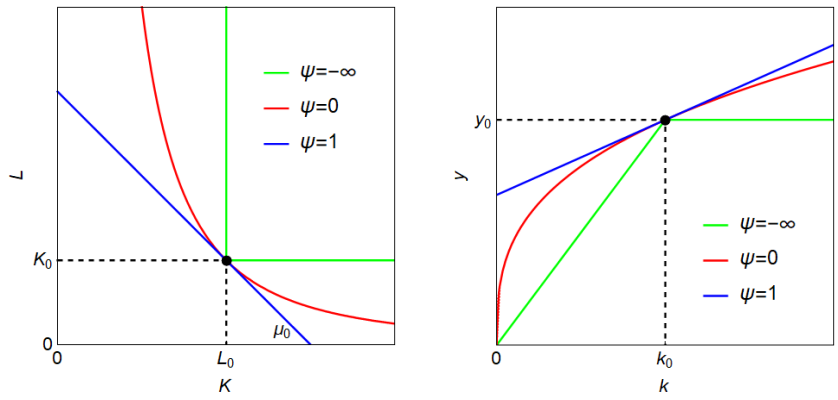

(A) Extensive forms (B) Intensive forms

Figure 1. Special cases of the normalized CES production function

3 Delay Solow Model

The fundamental equation of capital accumulation in the Solow model is described by a one-dimensional differential equation,

$$\dot{k}(t) = sf(k(t)) - (n + \delta)k(t) \tag{10}$$

where $k(t)$ is the per-capita capital at time t, $f(k)$ is the intensive form of the CES production function given in (9), $s \in (0,1)$ the constant marginal propensity to consume, $\delta \in (0,1)$ the depreciation rate of the capital and $n \in (0,1)$ the growth rate of population (that is, employment in the neoclassical framework). We introduce delays in this dynamic equation to see how the delays affect the growth of the economy. To this end, we adopt the delay capital accumulation equation formulated by Guerrini et al (2019) in which the Cobb-Douglas production function is used,

$$\dot{k}(t) = sf(k(t-\tau_1)) - (n+\delta)k(t-\tau_2) \tag{11}$$

where τ_1 is called a gestation delay and τ_2 a depreciation delay.[4] This section is divided into three subsections and consider the following cases: the no-delay case (i.e., $\tau_1 = \tau_2 = 0$) as a benchmark, the one-delay case (i.e., $\tau_1 > 0$ and $\tau_2 = 0$)[5] and finally the equal-delay case (i.e., $\tau_1 = \tau_2 = \tau$). The case of two different delays will be studied in the next section.

3.1 No Delays

The fundamental capital accumulation dynamics without delays is described by (10). For simplicity, let θ be the sum of n and δ. A steady state with $\dot{k}(t) = 0$ is reached when the capital intensity k^* solves the following:

$$\frac{f(k)}{k} = \frac{\theta}{s} \tag{12}$$

or

$$k^* = \left(\frac{1-\pi_0}{\left(\frac{k_0}{y_0}\frac{\theta}{s}\right)^{\psi} - \pi_0} \right)^{\frac{1}{\psi}}. \tag{13}$$

As is well-known, $\dot{k}(t) = 0$ implies that at the steady state, all of the investment is used to complement depreciation of the existing capital stock and additional capital for the incoming population.

Before proceeding we confirm how the equilibrium capital depends on the parameter ψ, which measures the elasticity of substitution between L and K. The average product of capital, the left-hand side of equation (12), is rewritten as

$$\frac{f(k)}{k} = y_0 \left[\frac{\pi_0}{(k_0)^{\psi}} + \frac{1-\pi_0}{k^{\psi}} \right]^{\frac{1}{\psi}}$$

and its derivative is negative in k for all values of ψ,

$$\frac{d}{dk}\left(\frac{f(k)}{k}\right) = -(1-\pi_0)\frac{f(k)/k}{\pi_0\left(\frac{k}{k_0}\right)^{\psi} + (1-\pi_0)} < 0.$$

[4] See Guerrini et al. (2019) for justification for the different length of the depreciation delay from that of the gestation delay.

[5] Since the other one-delay case of $\tau_1 = 0$ and $\tau_2 > 0$ is unrealistic from the economic point of view, we omit it.

Consider, first, the case of high elasticity of substitution with $0 < \psi < 1$ and then turn to the case of low elasticity of substitution with $\psi < 0$.[6]

Case I: $0 < \psi < 1$

The limits of the average product are

$$\lim_{k\to\infty} g(k,\psi) = \gamma(\psi) > 0$$

with

$$g(k,\psi) = \frac{f(k)}{k} \text{ and } \gamma(\psi) = \frac{y_0}{k_0}(\pi_0)^{\frac{1}{\psi}} > 0$$

and

$$\lim_{k\to 0} g(k,\psi) = \infty.$$

Given ψ, the average product is downward-sloping and is asymptotic to the positive constant, $\gamma(\psi)$. If θ/s is large enough so that

$$\frac{\theta}{s} > \gamma(\psi), \tag{14}$$

then equation (12) has a solution k^*, as seen in Figure 2. Given the parameter values as $\psi_A = 1/2$, $\pi_0 = 1/3$, $y_0 = k_0 = 1/2$, the graph of the average product $g(k)$ against positive k is illustrated as the downward sloping curve in the first quadrant and the graph of $\gamma(\psi)$ against positive ψ is depicted as the positive sloping curve in the second quadrant.[7] Notice that

$$\gamma(1) = \frac{y_0\pi_0}{k_0} \text{ and } \lim_{\psi\to 0}\gamma(\psi) = 0.$$

If the direction of the inequality in (14) is reversed, then $g(k) > \theta/s$ holds for only $k \geq 0$ and the sustainable growth (i.e., $\dot{k}(t) > 0$) takes place. It is apparent from Figure 2 that a stronger sufficient condition for the existence of the equilibrium is

$$\frac{\theta}{s} > \gamma(1)$$

under which the equilibrium capital always exists in the high elasticity of substitution case.

[6] See Klump and Preissler (2000) for more detail.

[7] Please observe that we cut and paste two different figures to construct Figure 2.

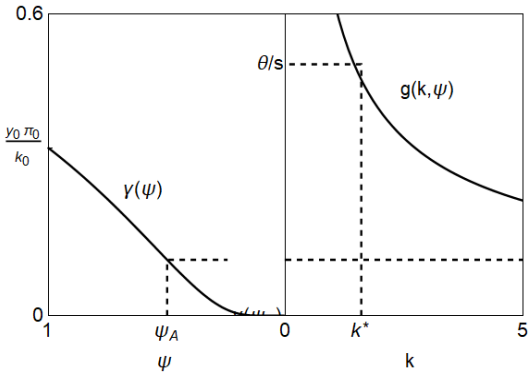

Figure 2. Determination of $k^* : 0 < \psi < 1$

Case II: $\psi < 0$

The average product approaches zero as k increases infinitely and converges to some positive constant as k goes to zero,

$$\lim_{k\to\infty} g(k,\psi) = 0$$

and

$$\lim_{k\to 0} g(k,\psi) = \gamma(\psi) > 0.$$

If θ/s is small enough so that

$$\frac{\theta}{s} < \gamma(\psi), \tag{15}$$

then equation (12) has the solution as seen in Figure 3 in which the graph of $g(k)$ is illustrated in the first quadrant as in Figure 2 while the graph of $\gamma(\psi)$ against negative ψ is depicted as a downward sloping curve in the second quadrant. If condition (15) is violated, then $g(k) - \theta/s < 0$ for all k and the capital stock declines continuously. Notice that

$$\lim_{\psi\to 0} \gamma(\psi) = \infty \text{ and } \lim_{\psi\to -\infty} \gamma(\psi) = \frac{y_0}{k_0}.$$

A stronger sufficient condition for the existence of the equilibrium capital stock is

$$\frac{\theta}{s} < \frac{y_0}{k_0}$$

under which the equilibrium capital always exists in the low elasticity of substitution case.

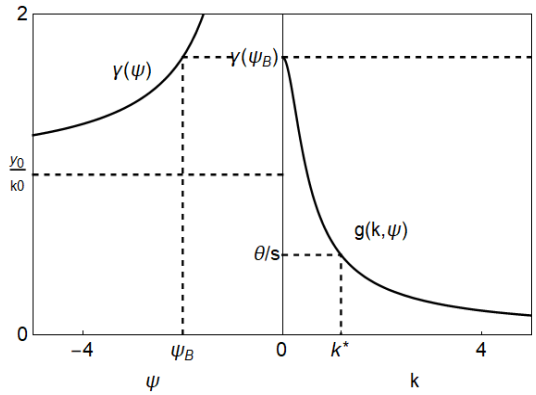

Figure 3. Determination of $k^* : \psi < 0$

Since $f(k)/k$ strictly decreases, $f'(k)k - f(k) < 0$ so at the steady state,

$$f'(k^*) < \frac{f(k^*)}{k^*} = \frac{\theta}{s}.$$

Therefore if π^* denote the capital share at the steady state, then

$$\pi^* = \frac{f'(k^*)k^*}{f(k^*)} < \frac{\theta k^*}{sf(k^*)} = 1.$$

To check the local stability at the equilibrium, we linearize the accumulation equation in the neighborhood of the equilibrium

$$\dot{k}(t) = [sf'(k^*) - \theta]\, k(t) \tag{16}$$

where

$$sf'(k^*) - \theta < 0.$$

Hence the eigenvalue of the linearized equation is negative. Summarizing the result yields the followings:

Theorem 1 *If either $\theta/s > \gamma(\psi)$ for $0 < \psi < 1$ or $\theta/s < \gamma(\psi)$ for $\psi < 0$, then the equilibrium $k^* > 0$ exists and is locally asymptotically stable.*

3.2 One Delay

Suppose that there is only an gestation delay, $\tau > 0$, of investment in the capital accumulation, which Kalecki (1935) considers for his macroeconomic dynamic study,

$$\dot{k}(t) = sf(k(t-\tau)) - \theta k(t) \tag{17}$$

where k^* in (13) is also a stationary point. The linearized system is

$$\dot{k}(t) = \theta\pi^* k(t-\tau) - \theta k(t)$$

where

$$sf'(k^*) = \theta\pi^*$$

The corresponding characteristic equation is

$$\lambda - \theta\pi^* e^{-\lambda\tau} + \theta = 0. \tag{18}$$

Assume that $\lambda = i\omega$ with $\omega > 0$. The real and imaginary parts of the characteristic equation are

$$\theta\pi^* \cos\omega\tau = \theta$$

and

$$\theta\pi^* \sin\omega\tau = -\omega.$$

Squaring both sides of these equations and adding them give

$$\omega^2 = \theta^2 (\pi^* + 1)(\pi^* - 1) < 0.$$

Hence there is no $\omega > 0$ satisfying the characteristic equation (18). No stability change to instability from stability occurs. This result has been already confirmed in the case of a Cobb-Douglas production function (see Guerrini et at. (2019), Lemma 2). We confirm it under the normalized CES production function, implying that the gestation delay is harmless to the stability of the balanced growth equilibrium.

Theorem 2 *The equilibrium point k^* of the one delay capital accumulation equation (17) is locally asymptotically stable for any $\tau > 0$.*

3.3 Equal-Delays

Since $\tau_1 = \tau_2 = \tau$ is assumed, the delay dynamic equation (11) can be written as

$$\dot{k}(t) = sf(k(t-\tau)) - \theta k(t-\tau) \tag{19}$$

where, again, k^* in (13), is a stationary point. The equal-delays means that the capital depreciation starts when the capital becomes productive. The linearized equation is obtained as

$$\dot{k}(t) = -(1-\pi^*)\theta k(t-\tau).$$

Suppose this equation has an exponential solution,

$$k(t) = e^{\lambda t} u.$$

The corresponding characteristic equation is written as

$$\lambda + (1 - \pi^*)\, \theta e^{-\lambda \tau} = 0. \tag{20}$$

Substituting the exponential solution into the characteristic equation (20) and separating the real and imaginary parts yield two equations,

$$(1 - \pi^*)\, \theta \cos \omega \tau = 0$$

and

$$\omega - (1 - \pi^*)\, \theta \sin \omega \tau = 0.$$

Squaring both sides of these equations and adding them give

$$\omega^2 = (1 - \pi^*)^2\, \theta^2 > 0.$$

The critical values τ that satisfy these two equations are

$$\tau^\ell(\psi) = \frac{1}{(1 - \pi^*(\psi))\, \theta} \left[\frac{\pi}{2} + 2\ell\pi\right] \text{ for } \ell = 0, 1, 2, ... \tag{21}$$

The direction of stability switches can be determined as follows. Consider λ as a function of τ, the bifurcation parameter, and differentiate the characteristic equation (20) with respect to τ,

$$\lambda' + (1 - \pi^*)\, \theta e^{-\lambda \tau} \left(-\lambda' \tau - \lambda\right) = 0$$

implying that

$$\lambda' = \frac{-\lambda^2}{1 + \lambda \tau}$$

where the characteristic equation is used to derive this form. If $\lambda = i\omega$, then

$$\lambda' = \frac{\omega^2 - i\tau\omega^3}{1 + \tau^2 \omega^2}$$

with a positive real part. So at the smallest critical value $\tau^0(\psi)$, stability is lost, and it cannot be regained with larger values of τ. Hence, the results obtained in the case of the equal delays are summarized as follows:

Theorem 3 *The equilibrium point k^* of the equal-two-delay equation (19) exists and is locally asymptotically stable for $\tau < \tau^0(\psi)$, loses stability at $\tau = \tau^0(\psi)$ and bifurcates to a limit cycle for $\tau > \tau^0(\psi)$.*

Under Assumption 1 with $\theta = 1/10$, $s = 1/5$ and $\ell = 0$, the stability switching curve against ψ is obtained as a positive sloping curve as illustrated in Figure 4(A). The steady state is locally asymptotically stable for τ less than $\tau^0(\psi)$, that is, τ in the yellow region. The horizontal dotted line is the limit of $\tau^0(\psi)$ as ψ goes to negative infinity (the limit is 5π). For $\psi_a = -1$, the critical value is

$$\tau^0(\psi_a) = 6\pi \simeq 18.85.$$

It is seen in Figure 4(A) that the steady state loses its stability at the red point on the stability switching curve (i.e., $\tau = 6\pi$) and in Figure 4(B) that it bifurcates to a limit cycle as a value of τ becomes larger than the critical value.

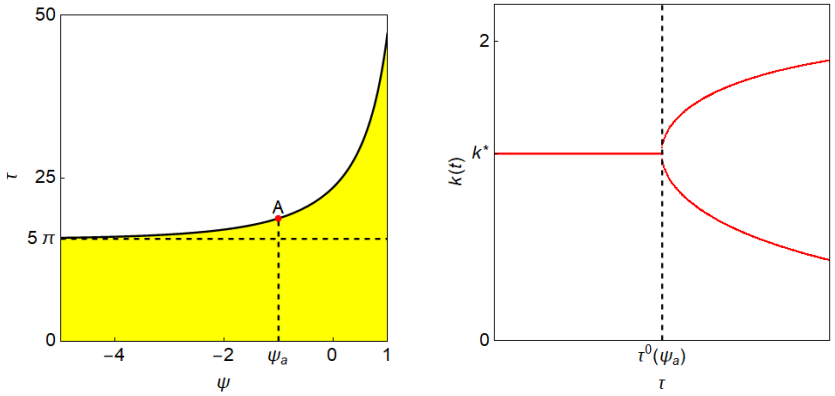

(A) Stability region (B) Bifurcation diagram

Figure 4. Stability switching and the birth of a limit cycle.

4 Solow Model with Two Different Delays

This section is also divided into three subsections. The stability switching curve with two delays is analytically obtained in Section 4.1. The stability index on the stability switching curve is determined in Section 4.2. Finally, in Section 4.3, three examples numerically confirm the analytical results.

4.1 Construction of the Stability Switching Curve

We now consider the general case of $\tau_1 > 0$, $\tau_2 > 0$ and $\tau_1 \neq \tau_2$. For convinence, we restate the delay capital accumulation equation:

$$\dot{k}(t) = sf(k(t-\tau_1)) - (n+\delta)k(t-\tau_2). \tag{22}$$

To study the stability change when τ_1 and τ_2 can vary, we will follow the methodology of Gu et al. (2005) with the use of the stability switching curve.

To apply this method, we first differentiate dynamic equation (22) with respect to delay variables and then obtain the linearized version of (22) evaluated at the equilibrium state k^*,

$$\dot{k}(t) = \theta\pi^* k(t-\tau_1) - \theta k(t-\tau_2) \tag{23}$$

where, from the definition of the equilibrium share of capital and from linearized equation (23),

$$sf'(k^*) = \theta\pi^*.$$

With an exponential solution, $k(t) = e^{\lambda t}u$, the characteristic equation is

$$a(\lambda, \tau_1, \tau_2) = 1 + a_1(\lambda)e^{-\lambda\tau_1} + a_2(\lambda)e^{-\lambda\tau_2} = 0 \tag{24}$$

where

$$a_1(\lambda) = -\frac{\theta\pi^*}{\lambda} \text{ and } a_2(\lambda) = \frac{\theta}{\lambda}.$$

For each $\lambda = i\omega$, the term $a(i\omega, \tau_1, \tau_2)$ in the complex plane is represented as the sum of three vectors, 1, $a_1(i\omega)e^{-i\omega\tau_1}$ and $a_2(i\omega)e^{-i\omega\tau_2}$, with magnitudes 1, $|a_1(i\omega)|$ and $|a_2(i\omega)|$, respectively. If these vectors create a triangle (i.e., $a(i\omega, \tau_1, \tau_2) = 0$), then the characteristic equation has a solution for some delays, τ_1 and τ_2. Since the length of each side of a triangle cannot exceed the sum of the lengths of the remaining two sides, we have the following three inequalities:

$$|a_1(i\omega)| + |a_2(i\omega)| \geq 1 \text{ and } -1 \leq |a_1(i\omega)| - |a_2(i\omega)| \leq 1. \tag{25}$$

which are called the triangle conditions. Figure 5 illustrates a triangle that satisfies the conditions (25).

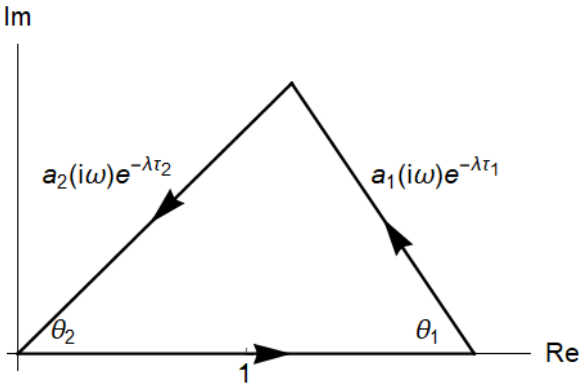

Figure 5. Triangle conditions

For $\lambda = i\omega$ with $\omega > 0$, these vectors are

$$a_1(i\omega) = i\pi^*\frac{\theta}{\omega} \text{ and } a_1(i\omega) = -i\frac{\theta}{\omega},$$

their absolute values are

$$|a_1(i\omega)| = \pi^* \frac{\theta}{\omega} \text{ and } |a_2(i\omega)| = \frac{\theta}{\omega},$$

and their arguments are

$$\arg\left[a_1(i\omega)\right] = \frac{\pi}{2} \text{ and } \arg\left[a_3(i\omega)\right] = -\frac{3\pi}{2}.$$

The triangle conditions give an interval of ω,

$$I = \left[(1-\pi^*)\,\theta, (1+\pi^*)\,\theta\right]. \tag{26}$$

For any $\omega \in I$, the characteristic equation has a pair of pure imaginary roots. In Figure 5, θ_1 and θ_2 represent the internal angles of the triangle and are determined by the law of cosine as follows:

$$\theta_1(\omega) = \cos^{-1}\left[\frac{\omega^2 - \left(1-\pi^{*2}\right)\theta^2}{2\pi^*\theta\omega}\right]$$

and

$$\theta_2(\omega) = \cos^{-1}\left[\frac{\omega^2 + \left(1-\pi^{*2}\right)\theta^2}{2\theta\omega}\right].$$

It is possible to identify solutions (τ_1, τ_2) of $a(i\omega, \tau_1, \tau_2) = 0$ that satisfy the following equations,

$$\left\{\arg\left[a_1(\omega)e^{-i\omega\tau_1}\right] + 2m\pi\right\} \pm \theta_1(\omega) = \pi$$

and

$$\left(\arg\left[a_2(\omega)e^{-i\omega\tau_2}\right] + 2n\pi\right) \mp \theta_2(\omega) = \pi.$$

Two cases appear in these equations, since the triangle can be placed above and under the horizontal axis. Solving them for τ_1 and τ_2 yields, for integers m and n,

$$\tau_1^{\pm}(\omega, m) = \frac{1}{\omega}\left[\frac{\pi}{2} + (2m-1)\pi \pm \theta_1(\omega)\right] \tag{27}$$

and

$$\tau_2^{\mp}(\omega, n) = \frac{1}{\omega}\left[\frac{3\pi}{2} + (2n-1)\pi \mp \theta_2(\omega)\right]. \tag{28}$$

Let $\boldsymbol{B}$ and $\boldsymbol{R}$ be the pair of the delays defined as

$$\boldsymbol{B} = \left\{\left(\tau_1^+(\omega, m), \tau_2^-(\omega, n)\right) \mid \omega \in I,\ m, n \in \mathbb{Z}\right\}$$

and

$$\boldsymbol{R} = \left\{\left(\tau_1^-(\omega, m), \tau_2^+(\omega, n)\right) \mid \omega \in I,\ m, n \in \mathbb{Z}\right\}.$$

Then we have the following:

Theorem 4 *The stability switching curves are given as*

$$T = \boldsymbol{B} \cup \boldsymbol{R}. \tag{29}$$

This is the set of all τ_1 and τ_2 such that $a(i\omega, \tau_1, \tau_2) = 0$ on which the characteristic equation has a purely imaginary root, $\lambda = i\omega$ with $\omega > 0$.

4.2 Stability Index

In order to find the directions of stability switches, we first compute

$$a_1(i\omega)e^{-i\omega\tau_1} = i\frac{\pi^*\theta}{\omega}\left(\cos\omega\tau_1 - i\sin\omega\tau_1\right)$$

and

$$a_2(i\omega)e^{-i\omega\tau_2} = -i\frac{\theta}{\omega}\left(\cos\omega\tau_2 - i\sin\omega\tau_2\right)$$

with real and imaginary parts

$$R_1 = \mathrm{Re}\left[a_1(i\omega)e^{-i\omega\tau_1}\right] = \frac{\pi^*\theta}{\omega}\sin\omega\tau_1,$$

$$I_1 = \mathrm{Im}\left[a_1(i\omega)e^{-i\omega\tau_1}\right] = \frac{\pi^*\theta}{\omega}\cos\omega\tau_1$$

and

$$R_2 = \mathrm{Re}\left[a_2(i\omega)e^{-i\omega\tau_2}\right] = -\frac{\theta}{\omega}\sin\omega\tau_2,$$

$$I_2 = \mathrm{Im}\left[a_2(i\omega)e^{-i\omega\tau_2}\right] = -\frac{\theta}{\omega}\cos\omega\tau_2.$$

Then the stability index is defined as

$$\begin{aligned} Q &= R_2I_1 - R_1I_2 \\ &= \frac{\pi^*\theta^2}{\omega^2}\left[\sin\omega\tau_1\cos\omega\tau_2 - \sin\omega\tau_2\cos\omega\tau_1\right]. \end{aligned}$$

By the addition theorem,

$$Q = \frac{\pi^*\theta^2}{\omega^2}\sin\left[\omega\left(\tau_1 - \tau_2\right)\right] \tag{30}$$

which has the same sign as $\sin\left[\omega\left(\tau_1 - \tau 2\right)\right]$.

We call the direction of the stability switching curve that corresponds to increasing ω the *positive direction*. We also call the region on the left-hand (right-hand) side of the stability switching curve the *region on the left* (*right*) when we head in the positive direction of the curve. We are now ready to mention the stability loss and gain on the stability switching curve. If $Q \neq 0$, then we have the following result from Theorem A.2 of Matsumoto and Szidarovszky (2018):

Theorem 5 *Let $\omega \in I$ such that $i\omega$ is a simple pure complex eigenvalue. At a point (τ_1, τ_2), we look toward increasing values of ω. As (τ_1, τ_2) moves from the region on the right to the left of the corresponding curve of T, a pair of eigenvalues cross the imaginary axis to the right if $Q > 0$. If $Q < 0$, then the crossing is in the opposite direction.*

If $Q = 0$, then Theorem 5 does not indicate the direction of the stability switches. This is the case when $\omega(\tau_1 - \tau_2) = k\pi$ with an integer k. Then $-\omega\tau_2 = k\pi - \omega\tau_1$, hence at $\lambda = i\omega$, the characteristic equation becomes

$$i\omega - \pi^*\theta e^{-i\omega\tau_1} + \theta e^{ik\pi} e^{-i\omega\tau_1} = i\omega - \theta\left(\pi^* - e^{ik\pi}\right) e^{-i\omega\tau_1} = 0. \tag{31}$$

Notice that

$$e^{ik\pi} = \cos k\pi + i \sin k\pi = \begin{cases} 1 \text{ if } k \text{ is even,} \\ -1 \text{ if } k \text{ is odd.} \end{cases}$$

Introduce the notation,

$$A(k) = \begin{cases} \theta(\pi^* - 1) < 0 \text{ if } k \text{ is even,} \\ \theta(\pi^* + 1) > 0 \text{ if } k \text{ is odd,} \end{cases}$$

since $\pi^* < 1$. Then from (31),

$$i\omega - (\cos\omega\tau_1 - i \sin\omega\tau_1) A(k) = 0.$$

Separating the real and imaginary parts,

$$A(k) \cos\omega\tau_1 = 0$$

and

$$A(k) \sin\omega\tau_1 = -\omega.$$

Hence

$$\cos\omega\tau_1 = 0 \text{ and } \sin\omega\tau_1 = -\frac{\omega}{A(k)} = \begin{cases} 1 \text{ if } k \text{ is even,} \\ -1 \text{ if } k \text{ is odd,} \end{cases}$$

and therefore,

$$\omega = \begin{cases} -A(k) = \theta(\pi^* - 1) < 0 \text{ if } k \text{ is even,} \\ A(k) = \theta(\pi^* - 1) > 0 \text{ if } k \text{ is odd.} \end{cases}$$

These values correspond to the end points of the interval $I\!I$. So $Q = 0$ holds at the initial and endpoints of the different segments of T, implying that stability switch cannot occur inside the segments. Hence the direction has to be the same as at the segments starting or ending at this point.

4.3 Three Examples

Solow (1956) confirms his analytical results by working out three numerical examples in which the production function is specified as a Leontief type, a Cobb-Douglas type or a CES type. In the same way, we examine three examples to see how the two delays affect the balanced growth.

Example 1: Leontief technology.

We first take $\psi = -5$ with which the CES production function (9) might approximate the Leontief function. The corresponding stability switching curve is described by the blue-red segments in Figure 6(A) in which the blue segments belong to $\boldsymbol{B}$ of (29) and so do the red segments to $\boldsymbol{R}$. More precisely,

$$\boldsymbol{B} = \boldsymbol{B}_0 \cup \boldsymbol{B}_1 \text{ and } \boldsymbol{R} = \boldsymbol{R}_1 \cup \boldsymbol{R}_2$$

where the four segments are defined as follows, as the vertical shift parameter n is fixed at $n = 0$ and the horizontal shift parameter m increases from 0 to 2 with a unit increment,

$$\boldsymbol{B}_i = \left\{ \left(\tau_1^+(\omega, i), \tau_2^-(\omega, 0) \right) \right\} \text{ for } i = 0, 1 \tag{32}$$

and

$$\boldsymbol{R}_j = \left\{ \left(\tau_1^-(\omega, j), \tau_2^+(\omega, 0) \right) \right\} \text{ for } j = 1, 2. \tag{33}$$

$\boldsymbol{B}_0$ is the left-most blue segment and $\boldsymbol{R}_1$ is next to the right of $\boldsymbol{B}_0$. The arrows on the blue and red segments indicate the positive directions of the corresponding segments.

Let us calculate the stability index on the segments. By (30), the stability index on the segments $\boldsymbol{B}$, denoted by $Q_{\boldsymbol{B}}$, is

$$Q_{\boldsymbol{B}} = \frac{\pi^* \theta^2}{\omega^2} \sin \left[\omega \left(\tau_1^+(\omega) - \tau_2^-(\omega) \right) \right]. \tag{34}$$

By (27) with $m = 0, 1, 2$ and (28) with $n = 0$,

$$\sin \left[\omega \left(\tau_1^+(\omega) - \tau_2^-(\omega) \right) \right] = -\sin \left[\theta_1(\omega) + \theta_2(\omega) \right] \leq 0$$

where the inequality is due to $0 \leq \theta_1(\omega) + \theta_2(\omega) \leq \pi$. Similarly, the stability index on the segments $\boldsymbol{R}$, denoted by $Q_{\boldsymbol{R}}$, is

$$Q_{\boldsymbol{R}} = \frac{\pi^* \theta^2}{\omega^2} \sin \left[\omega \left(\tau_1^-(\omega) - \tau_2^+(\omega) \right) \right] \tag{35}$$

where

$$\sin \left[\omega \left(\tau_1^-(\omega) - \tau_2^+(\omega) \right) \right] = \sin \left[\theta_1(\omega) + \theta_2(\omega) \right] \geq 0.$$

Hence we have $Q_{\boldsymbol{B}} < 0$ on the blue segments and $Q_{\boldsymbol{R}} > 0$ on the red segments in Figure 6(A) in which the blue R_i and L_i for $i = 0, 1$ denote the region on the right and the region on the left with respect to the blue segments and so do the red R_j and L_j for $j = 1, 2$ with respect to the red segments. The stability switching curve divides the nonnegative region of (τ_1, τ_2) into two. When a pair of (τ_1, τ_2) moves from the lower region to the upper region, the stability is lost, according to Theorem 5.

Let next check the stability change at the connecting points of $\boldsymbol{B}_i$ and $\boldsymbol{R}_j$. It is seen in Figure 6(A) that $\boldsymbol{B}_0$ and $\boldsymbol{R}_1$ start at point S_0. Hence, it is the starting point of both segments,

$$S_0 = (\tau_1^a, \tau_2^a) = \boldsymbol{B}_0 \cap \boldsymbol{R}_1$$

with

$$\tau_1^a \simeq 15.87,\ \tau_2^a \simeq 15.87 \text{ and } \tau_1^a/\tau_2^a = 1.$$

In the same way, it is observed that point E_1 is the ending point of segments $\boldsymbol{B}_1$ and $\boldsymbol{R}_1$,

$$E_1 = \left(\tau_1^b, \tau_2^b\right) = \boldsymbol{B}_1 \cap \boldsymbol{R}_1$$

with

$$\tau_1^b \simeq 46.64,\ \tau_2^b \simeq 15.55 \text{ and } \tau_1^b/\tau_2^b = 3.$$

and point S_1 is the starting point of segments $\boldsymbol{B}_1$ and $\boldsymbol{R}_2$,

$$S_1 = (\tau_1^c, \tau_2^c) = \boldsymbol{B}_1 \cap \boldsymbol{R}_2$$

with

$$\tau_1^c \simeq 79.37,\ \tau_2^c \simeq 15.87 \text{ and } \tau_1^c/\tau_2^c = 5.$$

The ratio τ_1/τ_2 is an odd integer so that $Q = 0$ and the direction of stability is the same as that on the segment $\boldsymbol{B}_i$ or $\boldsymbol{R}_j$.[8] Hence, when a value of τ_2 increases along the vertical dotted line at τ_1^a, τ_1^b or τ_1^c and then crosses the stability switching curve from below, stability is lost.

We perform a numerical simulation to see what dynamics the delay system (22) can generate. The equilibrium point is locally asymptotically stable for (τ_1, τ_2) below the curve and unstable for the pair above. At point A with $\tau_1^A = 20$ and $\tau_2^A \simeq 15.9$ on the red segment $\boldsymbol{R}_1$, stability is lost. The bifurcation diagram with respect to τ_2 is illustrated in Figure 6(B) in which τ_1 is fixed at τ_1^A and τ_2 increases from $\tau_2^{\min}$ to $\tau_2^{\max}$ with an increment of $(\tau_2^{\max} - \tau_2^{\min})/500$ along the vertical dotted black line where

$$\tau_2^{\min} = 14.9 \simeq \tau_2^A - 1 \text{ and } \tau_2^{\max} = 20.5 \simeq \tau_2^A + 4.6.$$

For each value of $\tau_2 \in \left[\tau_2^{\min}, \tau_2^{\max}\right]$, the delay dynamic equation (22) runs for $0 \le t \le T(= 20,000)$ and the local maximum and minimum values of τ_2 obtained from the data for $T - 500 \le t \le T$ are plotted against the selected value. As can be seen, the equilibrium point is locally asymptotically stable for $\tau_2 < \tau_2^A$, loses its stability at $\tau_2 = \tau_2^A$ and bifurcates to a limit cycle for $\tau_2 > \tau_2^A$. It is also seen that a cycle-doubling bifurcation[9] occurs at $\tau_2^B \simeq 18.44$ and so

[8] Notice that at S_0, the critical values are the same, $\tau_1^a = \tau_1^a$. Equation (21) can determine those values for $\psi = -5$ and $\ell = 0$.

[9] In a discrete dynamical system, Figure 6(A) is called the period-doubling bifurcation in which the period of a periodic cycle is doubled. In a continuous dynamical system, a limit cycle having two extrema is changed to a limit cycle having four extrema, implying the number of cycles is doubled. Hence we call it "cycle-doubling."

does a cycle-halving bifurcation at $\tau_2^C \simeq 20.02$ when τ_2 further increases.[10]

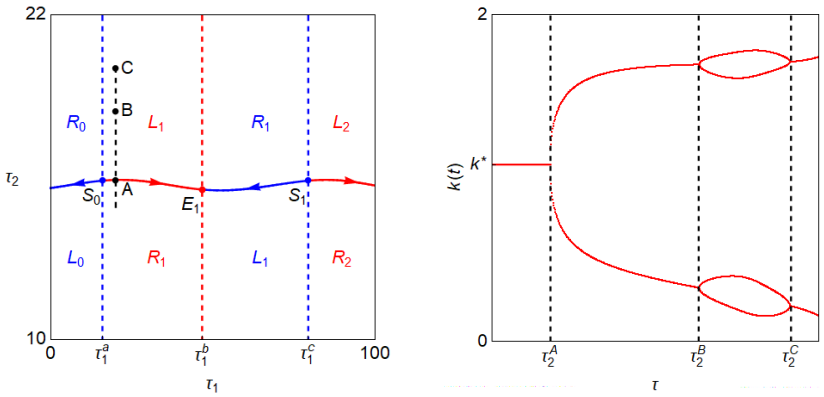

(A) Stability Region (B) BIfurcation diagram

Figure 6. Leontief technology

Example 2. Cobb-Douglas technology

We take $\psi = 1/10$ with which the CES production function (9) might approximate the Cobb-Douglas function. It is seen in Figure 7(A) that the stability switching curve takes a wave-like shape and its amplitude becomes larger than the tipple-like curve shown in Figure 6(A). Although the big waves are repeated, we limit value of τ_1 up to 50 in order to confine attention to the first wave. As in Example 1, we denote the blue segments by $\boldsymbol{B}_i$ for $i = 0, 1$ and the red segment by $\boldsymbol{R}_1$. Applying the formulas in (34) and (35), we find that $Q_{\boldsymbol{B}} < 0$ and $Q_{\boldsymbol{R}} > 0$. The blue R_i and L_i above and below the curve denote the regions on the right and the left along the blue segment while the red R_1 and L_1 denote the right and left region along the red segment. According to Theorem 5, the stability is lost when a pair of (τ_1, τ_2) crosses the blue segments from below to above. Although the red segment changes its slope from positive-sloping to negative sloping, the region on the left is located above the positive sloping part and on the right of the negative sloping part. Hence, the stability is lost when the pair of the delays moves from below to above or from left to right. The starting point of $\boldsymbol{B}_0$ and $\boldsymbol{R}_1$ is denoted as S_0 with

$$\tau_1^a \simeq 24.44,\ \tau_2^a \simeq 24.44 \text{ and } \tau_1^a/\tau_2^a = 1$$

and the ending point of $\boldsymbol{B}_1$ and $\boldsymbol{R}_1$ by E_1 with

$$\tau_1^b \simeq 34.72,\ \tau_1^b \simeq 11.57 \text{ and } \tau_1^b/\tau_1^b = 3.$$

Stability is lost when the pair of the delays passes these connection points from below to above.

[10] These bifurcation values are numerically obtained.

At point A on the blue segment $\boldsymbol{B}_0$, the boundary values are

$$\tau_1 = \tau_1^A = 20 \text{ and } \tau_2 = \tau_2^A \simeq 22.668$$

at which the equilibrium point loses stability. A limit cycle emerge from increasing τ_1 above τ_1^A as shown in Figure 7(B) in which the delay dynamic equation (22) runs for $0 \le t \le T(= 50,000)$ with the initial function $\varphi(t) = k^* - 0.1$ for $t \le 0$ and $(k(t), f(k(t)))$ for $T - 1000 \le t \le T$ is plotted. We take $\psi = \tau_2^A + 0.1$ for the small cycle, $\psi = \tau_2^A + 0.5$ for the medium cycle and $\psi = \tau_2^A + 1$ for the large cycle. The cycle is getting larger as the value of ψ increases. For a much larger value than $\tau_2^A + 1$, the nonnegative constraint of the per-capita capital may be violated.

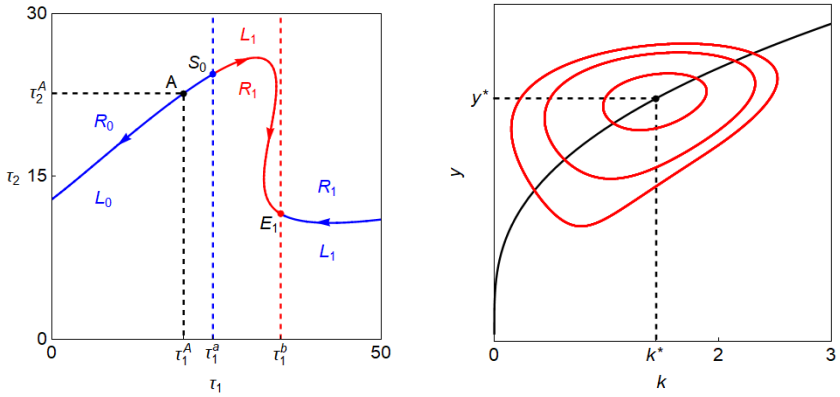

(A) Stability Region (B) Limit cycles

Figure 7. Cobb-Douglas technology

Example 3. CES technology with $\psi = 1/2$

The value of ψ is increased to $1/2$. This is the case considered by Solow (1956) in which two possibilities, endogenous steady-state growth and stable balanced growth, are numerically confirmed. We study another dynamic behavior of a delay CES economy. As can be seen in Figure 8(A), the larger value of ψ makes the red segment of the stability switching curve more winding than that in Figure 7(A). The region division and the stability-loss-and-gain are the same as those in Example 2. The starting point S_0 and the ending point E_1 have the following coordinates,

$$\tau_1^S \simeq 29.72,\ \tau_2^S \simeq 29.72 \text{ and } \tau_1^S/\tau_2^S = 1$$

and

$$\tau_1^E \simeq 32.03,\ \tau_2^E \simeq 10.68 \text{ and } \tau_1^E/\tau_2^E = 3.$$

Stability is lost when a pair of (τ_1, τ_2) crosses the blue segments from below to above. In addition, the more winding red segment generates a new phenomenon, multiple stability switches. The value of τ_2 is increased along the dotted vertical line standing at τ_1^A. The pair of (τ_1^A, τ_2) crosses the negative-sloping part of the red segment at point A from region R_1 to region $\underline{L}_1$ that means the lower left region. Since the stability index is positive (i.e., $Q_{\boldsymbol{R}} > 0$), Theorem 5 implies the loss of stability. With further increasing τ_2, the pair passes through point B on the positive-sloping part from below to above. Along the red segment, this is a movement from the left region (i.e.,. $\underline{L}_1$) to the right region (i.e., R_1), implying the gain of stability. Further increasing τ_2 brings the pair to point C on the flatter positive-sloping part, above which the upper left region $\overline{L}_1$ is. Going cross the point from below to above means the movement from the right region (i.e., R_1) to the left region (i.e., $\overline{L}_1$). With the positive stability index, we have the loss of stability again. No stability switch occurs afterward.

Let us see what dynamics the delay system (22) brings about when the stability is violated. It is numerically checked that an unstable trajectory exhibits expanding oscillations after point A until point B. Hence $k(t)$ sooner or later becomes zero, implying that the output production ceases and capital accumulation is terminated. It is also confined that the equilibrium point bifurcates to a limit cycle after point C (that is, for $\tau_2 > \tau_2^c$) as shown in Figure 8(B).

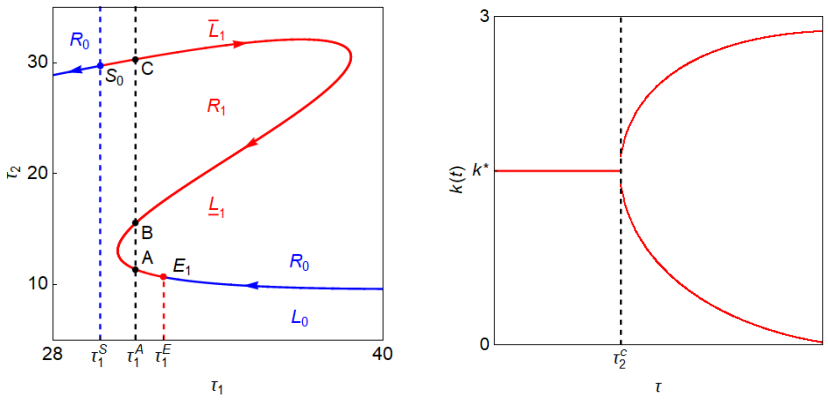

(A) Stability region (B) Bifurcation diagram

Figure 8. CES technology with $\psi = 1/2$

5 Concluding Remarks

This study characterizes the relation between the elasticity of factor substitution and the stability/instability of the steady state of a Solow model with two delays. Our main finding is that the multiple stability switching can occur if

the elasticity is high whereas multiple cyclic dynamics could be possible if the elasticity is low. The existence of more complex dynamics could be possible, however, not confirmed. It is interesting to apply the delay approach to different one-sector models of economic growth such as the Diamond overlapping generation model and the Keynesian model as well as to a two-sector growth model.

Appendix

In this Appendix, following Hicks (1963), we show the equivalence of the two definitions of the elasticity of substitution by Hicks (1932) and Robinson (1933). We transform the definition of σ_R to the that of σ_H under the conditions: only two inputs, homogeneity of degree one and perfect competition. With the production function with the degree one homogeneity and perfect competition, Euler's theorem says that the factors of production are paid according to their marginal productivities and then output exactly covers the factor payment,

$$Y = F_K K + F_L L \tag{A-1}$$

where $Y = F(K, L)$. Partially differentiating (A-1) with respect to K and L presents

$$F_{KK} K + F_{LK} L = 0 \tag{A-2}$$

and

$$F_{LL} L + F_{KL} K = 0. \tag{A-3}$$

From (2), the formulation of Robinson's definition is rewritten,

$$\sigma_R = \frac{d\left(\log K - \log L\right)}{d\left(\log F_L - \log F_K\right)} = \frac{dK/K - dL/L}{dF_L/F_L - dF_K/F_K} \tag{A-4}$$

The denominator of (A-4) can be developed as follows:

$$\begin{aligned} \frac{dF_L}{F_L} - \frac{dF_K}{F_K} &= \frac{F_{LL}dL + F_{LK}dK}{F_L} - \frac{F_{KK}dK + F_{KL}dL}{F_K} \\ &= \frac{F_{LL}F_K - F_{KL}F_L}{F_K F_L} dL - \frac{F_{KK}F_L - F_{LK}F_K}{F_K F_L} dK \end{aligned}$$

F_{LL} from (A-3) and F_{KK} from (A-2) are substituted in the second line of the above equation to obtain

$$\frac{F_{KL}}{F_K F_L} \left\{ \left(F_k K + F_L L\right) \frac{dK}{K} - \left(F_k K + F_L L\right) \frac{dL}{L} \right\} = \frac{F_{KL}}{F_K F_L} Y \left(\frac{dK}{K} - \frac{dL}{L} \right).$$

The last term is replaced with the denominator of (A-4) and then we arrive at Hicks' definition,

$$\sigma_R = \frac{F_K F_L}{F_{KL} Y} = \sigma_H.$$

References

Arrow. K., Chenery, H., Minhas, B., and Solow, R., Capital-labor substitution and economic efficiency, *Review of Economics and Statistics*, 43, 225-250, 1961.

Day, R., Irregular growth cycles, *American Economic Review*, 72, 406-414, 1982.

Goodwin, R., The nonlinear accelerator and the persistence of business cycles, *Econometrica*, 19,1-17, 1951.

Gori, L., Guerrini, L. and Sodini, M., Disequilibrium dynamics in a Keynesian model with time delays, *Communications in Nonlinear Science and Numerical Simulation*, 58, 10.101b/j.cnsns.2017.06.014.

Gu, K., Nicolescu, S., and Chen, J., On the stability crossing curve for general systems with two delays, *Journal of Mathematical Analysis and Applications*, 311, 231-253, 2005.

Guerrini, L., Matsumoto, A., and Szidarovszky, F., Neoclassical growth model with two fixed delays, *Metroeconomica*, doi:10.1111/meca 12257, 2019.

Hicks, J., *The Theory of Wages*, London, Macmillan, 1932.

Hicks, J., *A Contribution to the Theory of Trade Cycle*, London, Oxford University Press, 1950.

Hicks, J., *The Theory of Wages*, 2nd ed., London, Macmillan, 1963.

Kalecki, M., A macrodynamic theory of business cycles, *Econometrica*, 3, 327-344, 1935.

Klump, R., McAsam, P. and Willman A., The normalized CES production functions: theory and empirics, *Journal of Economic Surveys*, 26, 769-799, 2012.

Klump, R., and Preissler, H., CES production functions and economic growth, *Scandinavian Journal of Economics*, 102, 41-56, 2000.

Matsumoto, A. and Szidarovszky, F., Delay growth model with physical and human capitals, *Chaos, Solitons and Fractals*, 130, 109452, 2020.

Matsumoto, A. and Szidarovszky, F., *Dynamic Oligopolies and Time Delays*, Singapore, Springer Nature, 2018.

Matsumoto, A. and Szidarovszky, F., Delay differential neoclassical growth model, *Journal of Economic Behavior and Organization*, 78, 272-289, 2011.

Robinson, J., *The Economics of Imperfect Competition*, London, Macmillan, 1933.

Solow, R., A contribution to the theory of economic growth, *Quarterly Journal of Economics*, 70, 64-94, 1956.

Tsuzuki, E., Fiscal policy lag and equilibrium determinacy in a continuous-time new Keynesian model, *International Review of Economics*, 63, 215-232, 2016.